

SIGNATURES OF THE RISE OF CYCLE 23

W. A. DZIEMBOWSKI,^{1,2} P. R. GOODE,² A. G. KOSOVICHEV,³ AND J. SCHOU³

Received 1999 September 16; accepted 2000 February 15

ABSTRACT

During the rise of Cycle 23, we have found a sizable, systematic evolution of the *Solar and Heliospheric Observatory*/Michelson Doppler Imager solar oscillation frequencies implying significant changes in the spherically symmetric structure of the Sun's outer layers as well as in its asphericity up to a $P_{1.8}$ Legendre distortion. We conducted a search for corresponding asymmetries in Ca II K data from Big Bear Solar Observatory. We found tight temporal and angular correlations of the respective asphericities up through $P_{1.0}$. This result emphasizes the role of the magnetic field in producing the frequency changes. We carried out inversions of the frequency differences and the splitting coefficients assuming that the source of the evolving changes is a varying stochastic magnetic field. With respect to the most recent activity minimum, we detected a significant perturbation in the spherical part at a depth of 25–100 Mm, which may be interpreted as being a result of a magnetic perturbation, $\langle B^2 \rangle$, of about $(60\text{KG})^2$ and/or a relative temperature perturbation of about 1.2×10^{-4} . Larger, although less statistically significant, perturbations of the interior structure were found in the aspherical distortion.

Subject headings: Sun: interior — Sun: oscillations

1. INTRODUCTION

Helioseismic frequencies provide the most accurate global measures of cycle-dependent changes in the Sun. The advantages of a seismic investigation of the Sun include not only the prospect of seeing changes beneath the surface, but also deriving from the frequencies the surface-averaged parameters which quantify the Sun. The real challenge is to connect these global, seismic measures to observed characteristics of the dynamic Sun.

Deriving surface-averaged quantities from disk-averaged observations is a notoriously difficult matter. Here we faced the problem of absolute calibration using Big Bear Solar Observatory (BBSO) Ca II K data from full-disk observations. Making such a connection is critical to linking the Sun to other stars. Helioseismic measures are especially important here because they provide a unique opportunity to precisely measure surface averages (instead of disk averages).

The observed frequency changes of the solar oscillation multiplets are divided into centroid changes, which reflect surface-averaged changes in the Sun, and changes within the individual multiplets. The changes which are not symmetric about the multiplet centroid (the so-called even a -coefficients) show a strong cycle dependence. The direct source of the cycle-dependent changes has been a matter of controversy. However, the only well-established changes are dominated by effects arising in the outermost layers of the Sun.

We note that the symmetric part of the multiplet (about the centroid), the so-called odd a -coefficients, arises from the Sun's differential rotation. In this paper, we will not analyze or discuss this part of the data. Here we focus on

the part of the spectrum of the oscillation multiplets that shows appreciable cycle dependence.

The sources of the changes are considered to be some combination of variations in temperature, magnetic field, and changes in the random velocity field. Goldreich et al. (1991) proposed that changes in the superficial, random magnetic field are the primary cause of the centroid frequency shifts. This idea has been criticized by Kuhn (1998), who points out that Goldreich et al. require a mean, quadratic, near-surface magnetic perturbation, $\langle B^2 \rangle$, of around $(250\text{G})^2$, while the observations of Lin (1995) and Lin & Rimmele (1999) show a mean surface field which is significantly weaker. Instead, Kuhn sees a critical role for the variations of the turbulent pressure through the solar cycle. He proposes that changes in the aspherical component of the stresses are responsible for the varying even a -coefficients. This is plausible. However, there is strong evidence that both the centroid and even a frequency changes closely reflect changes in the magnetic field. In particular, we shall demonstrate here that the evolving asphericities in the even a 's are closely mimicked by the corresponding ones found in the BBSO Ca II K data. One possible way of evading the apparent contradiction Kuhn raises would be to contemplate a significant inward increase in the field intensity. We emphasize that in discussing the field, one has to be careful to distinguish between the direct mechanical effect of the Lorentz force and the thermal effect arising from the annihilation of the field (referred to as the β -effect) and the force's indirect effect on the thermal structure through the perturbation of the convective transport (referred to as the α -effect).

Clearly, we are lacking a basic understanding as to how the frequency changes arise. We need more observational information. The most crucial time period for which we need data is during the rise of the cycle from minimum. Fortunately, we have *Solar and Heliospheric Observatory* (SOHO) data covering that period for the current rising cycle. What we look for in these new data are higher order asymmetries, which we correlate with magnetic information from various sources. Furthermore, we look inside the

¹ Warsaw University Observatory and Copernicus Astronomical Center, Poland.

² Big Bear Solar Observatory, New Jersey Institute of Technology, 40386 North Shore Lane, Big Bear City, CA 92314.

³ W. W. Hansen Experimental Physics Laboratory, Stanford University.

varying Sun by inverting the frequency changes and the splitting coefficients.

2. FREQUENCY CHANGES FROM *SOHO*/MDI DATA

The data treated here consist of 12 72 day sets. The first 11 are consecutive and cover the period beginning 1996 May 1 and ending 1998 May 31. The last set (which is the first after the *SOHO* operation was recovered) covers 1999 February 3–1999 April 15. Each of the data points contains a centroid frequency, $\bar{\nu}_{l,n}$, and 36 splitting coefficients, a_k . Each set contains between 1620 and 1680 p -mode multiplets (of l -values from 1 to 200) and between 120 and 143 f -mode multiplets (of l -values from 123 to 300).

For each p -mode multiplet, the individual mode frequencies, $\nu_{l,n,m}$, are represented by

$$\nu_{l,n,m} - \bar{\nu}_{l,n} = \sum_{k=1} a_k \mathcal{P}_k^l(m), \quad (1)$$

where \mathcal{P} are orthogonal polynomials (see Ritzwoller & Lively 1991 and Schou, Christensen-Dalsgaard, & Thompson 1994). This representation ensures that $\bar{\nu}_{l,n}$ are a probe of the spherical structure, while a_{2k} —the even a -coefficients—are a probe of the symmetrical (about the equator) part of distortion described by the corresponding $P_{2k}(\cos \theta)$ Legendre polynomial. We have

$$\kappa_{kl}^m \equiv \int_0^{2\pi} \int_{-1}^1 |Y_l^m|^2 P_{2k} d(\cos \theta) d\phi = C_{kl} \mathcal{P}_{2k}^l(m), \quad (2)$$

where

$$C_{kl} = (-1)^k \frac{(2k-1)!!}{k!} \frac{(2l+1)!!}{(2l+2k+1)!!} \frac{(l-1)!}{(l-k)!}. \quad (3)$$

We separate the analyses of p - and f -modes because they have different properties in the outer layers. Our inferences

from the f -modes concern only possible variations in the seismic solar radius (see § 5). For the other sections of the paper, we consider only the centroid frequency of each p -mode and its attendant even a -coefficients.

The even-order splitting coefficients in each of the 12 data sets were fit to the following formula (Dziembowski & Goode 1991):

$$a_{2k(ln)} = a_{2k(ln)\text{rot}} + C_{kl} \frac{\gamma_k}{I_{ln}}, \quad (4)$$

where $a_{2k(ln)\text{rot}}$ represents the effect of centrifugal distortion, which we calculate from the *SOHO*/Michelson Doppler Imager (MDI) data following the treatment of Dziembowski & Goode (1992); I_{ln} is a measure of the modal inertia (also called the mode mass), and γ_k is the asphericity coefficient corresponding to a P_{2k} distortion. Since our plan is to study the temporal variation of the asymmetry, we eliminate the constant distortion of rotation from the γ -coefficients in equation (4). The modal inertia was evaluated assuming that all modes have the same radial displacement at the base of the solar photosphere. Adopting a value of 10^4 for that displacement, we have $I_{20,19} \approx 1$. The inertia decreases with increasing l or n . Equation (4) has also been used to represent changes in centroid frequencies. However, in that case we can determine only a relative γ_0 . For this, we chose the first of the 12 MDI sets as the reference.

The I_{ln}^{-1} factor accounts for most of the l and frequency dependence in the splitting coefficients. This result is due to Libbrecht & Woodard (1990). They used it as evidence that the asphericity responsible for the even a -coefficients is localized well above the lower turning point of modes in the sample, that is, close to the surface. Dziembowski & Goode (1991) were able to determine a slight, but significant ν dependence of the γ_1 and γ_2 coefficients from the same data. First, we present the results of fitting constant γ 's to each of

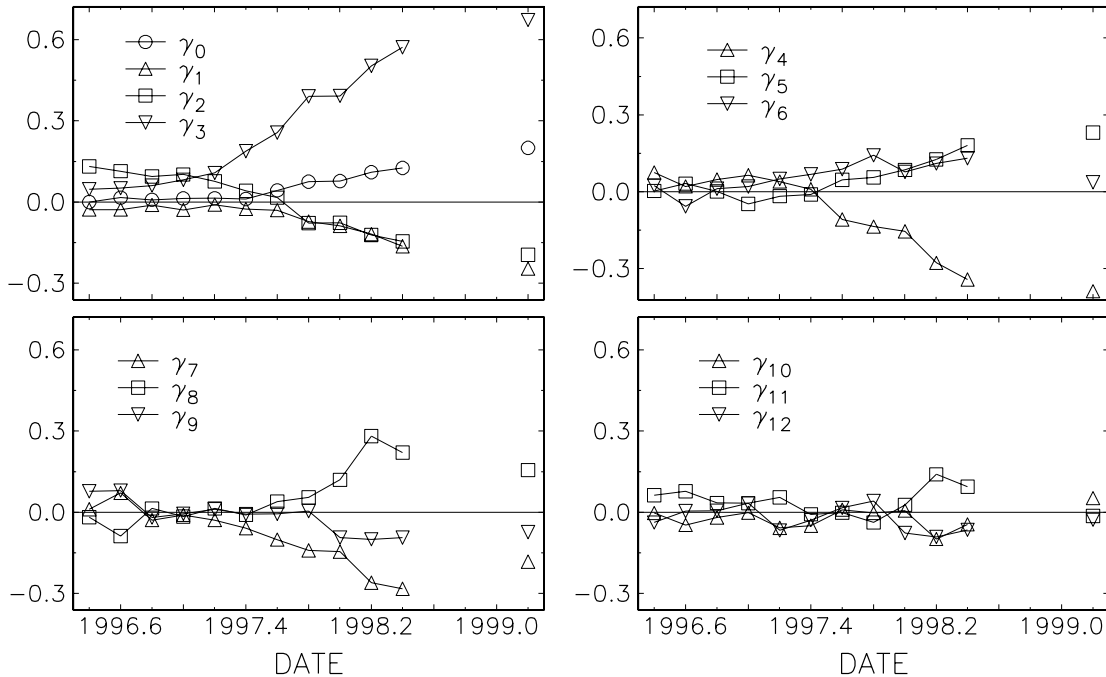


FIG. 1.—Mean asphericity coefficients, γ (in μHz), from the 12 *SOHO*/MDI 72 day sets. The first 11 were obtained consecutively during the first 2 years of *SOHO* observations (1996 May 1–1998 May 31). The 12th covers 1999 February 3–1999 April 15. For γ_0 – γ_6 , the error bars were within the symbols. The errors increase with order, but even for γ_{12} the error bars span only $4 \times 10^{-2} \mu\text{Hz}$.

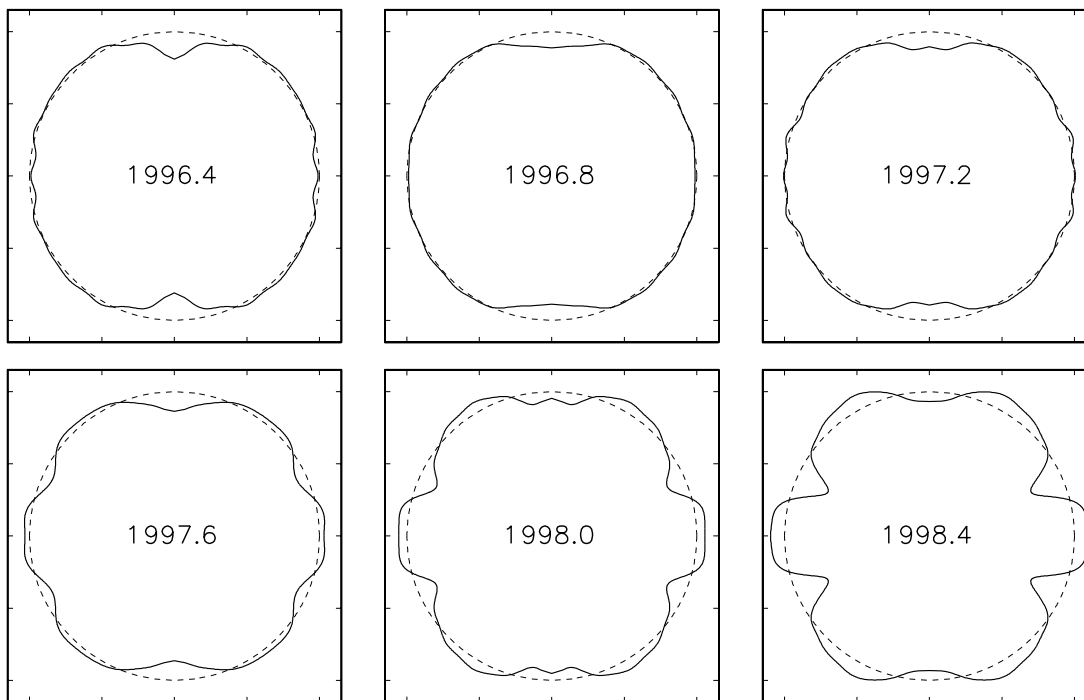


FIG. 2.—Temporal evolution of the solar asphericity over the first 2 years of MDI data analyzed here. The actual model asphericity is about 300,000 times smaller than shown.

the 12 sets of the even a -coefficients from the *SOHO*/MDI instrument.

In Figure 1, we show the first 12 γ -coefficients. This figure is a continuation of Figure 1 in Dziembowski et al. (1998). Here we have 12 72 day long sets, while previously we had only five. We now see clear trends in all four γ -coefficients— γ_0 , γ_1 , γ_2 , and γ_3 —whereas before there was

no clear trend in γ_0 . Furthermore, we now see clear trends in γ_4 and γ_5 . This is the first time that we see a significant trend in the asphericity beyond P_6 . Beyond P_{10} , there is not always a clear trend, although P_{14} and P_{16} are fairly suggestive. We note that the errors are rapidly increasing with order, k . In detail, the error bars through P_{12} are inside the symbol. The errors increase with order, but even for P_{24} the

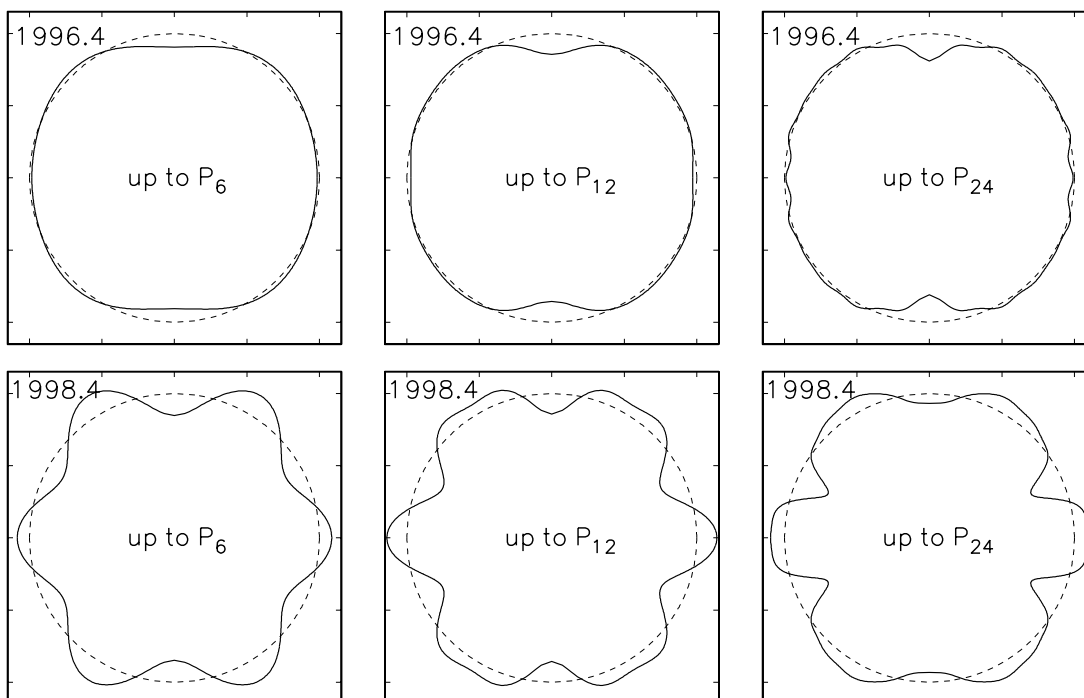


FIG. 3.—Cumulative contribution of the model asphericities over the first 2 years of MDI data. As in Fig. 2, the true model asphericities are amplified about 300,000 times.

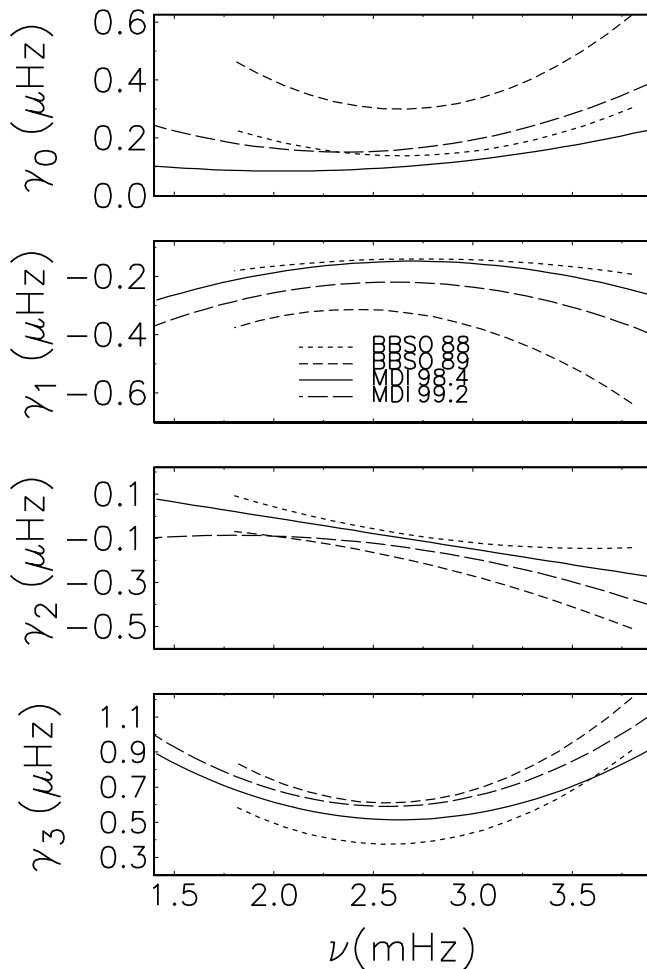


FIG. 4.— $\gamma(\nu)$ dependence of MDI data from the two most recent 72 day sets. Also shown for comparison are the BBSO data from 1988 and 1989.

error bars span only $4 \times 10^{-2} \mu\text{Hz}$. Even there, the values are marginally significant, although there is not a clear trend for P_{24} . Therefore, we focus our analysis on the first few coefficients in the expansion.

Bhatnagar, Jain, & Tripathy (1999) analyzed the centroid changes in the Global Oscillation Network Group (GONG) frequencies covering the period 1995 August–1997 August. They found an increasing tendency over a period comparable to that of our results. For characterizing the mean frequency change, they used the quantity

$$\overline{\Delta\nu} = \sum_{ln} \frac{I_{ln} \Delta\nu_{ln}}{\sigma_{ln}^2} \left(\sum_{ln} \frac{I_{ln}}{\sigma_{ln}^2} \right)^{-1},$$

where σ_m is the measurement error, and found the value of $0.023 \mu\text{Hz}$. From the MDI data covering the same period we derived $\overline{\Delta\nu} = 0.021 \mu\text{Hz}$. Note that the definition of $\overline{\Delta\nu}$ differs substantially from γ_0 , and that the γ 's are the proper characterization of mean frequency changes under the hypothesis that they arise near the surface.

Howe, Komm, & Hill (1999) used a lengthier string of GONG frequencies covering the period 1995 August–1998 August. In addition to centroid changes, they analyzed the splitting coefficients up to a_6 . They used a weighted average over modes near 3 mHz. Essentially, our results agree with theirs. In particular, after calculating the mean MDI frequency changes, according to their prescription, we found a

value of $0.21 \mu\text{Hz}$. This is to be compared with $0.25 \mu\text{Hz}$, as determined by Howe et al. (1999). Bearing in mind the fact that some interpolation of the MDI data was needed, we may say that the two numbers agree.

One of our basic problems here is relating the asymmetries seen in the oscillation frequency multiplets to those in the Sun. In Figure 2, we do this with a model and a caricature. The key to the model is noting that one can calculate the rotational distortion of the Sun and the corresponding asymmetry that would result in the spectrum of solar oscillations. Of course, centrifugal distortion is dominated by a P_2 shape distortion of the Sun, which turns out to correspond to a γ_1 of $0.037 \mu\text{Hz}$. Using this to scale all of the γ 's from the MDI data and multiplying the resulting distortions by about 300,000, we obtain Figure 2. In Figure 2, we show a caricature of the temporal evolution of the asphericity of the Sun implied by the γ 's of Figure 1. The relative roles of the lower and higher order distortions are illustrated in Figure 3. From this figure, it is clear that a low-order expansion gives at least a rough picture of the true asymmetry in the oscillation spectrum.

3. PREDICTION OF LOW-DEGREE MODE SPECTRUM FOR WHOLE DISK OBSERVATIONS

As described by Dziembowski & Goode (1997), the γ -coefficients from moderate l data can be used to accurately evaluate the frequency changes for low-degree modes under the assumption that the cycle-dependent perturbation is localized near the surface.

In Figure 4, we plot the frequency dependence of the γ 's as determined from a three-term polynomial fit. For comparison, we show the equivalent curve obtained from BBSO data from 1988 and 1989. From this, we see that the mid-

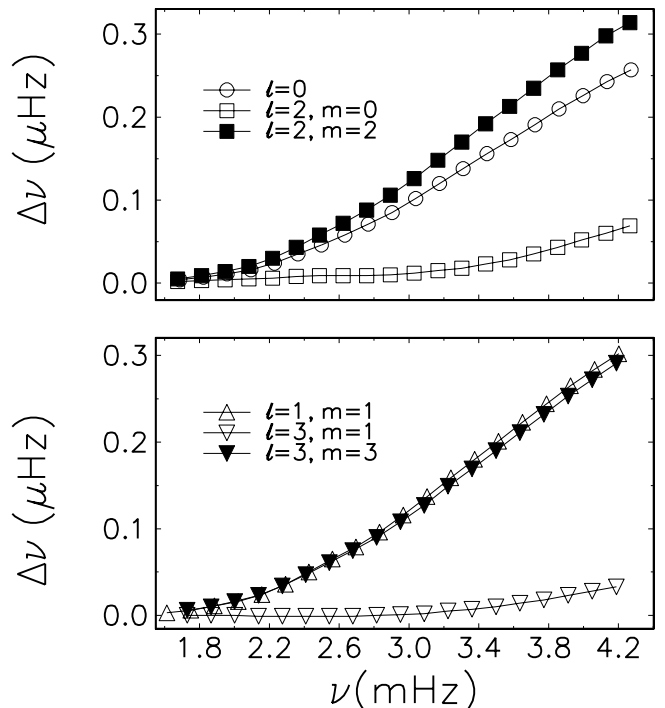


FIG. 5.—Upper panel: Predicted frequency shift, from MDI data, at 1998.4 for $l=0$ and 2 data as a function of frequency. Lower panel: The same for $l=1$ and 3. Note that for each (l, m) -mode, the perturbation is the same for m and $-m$.

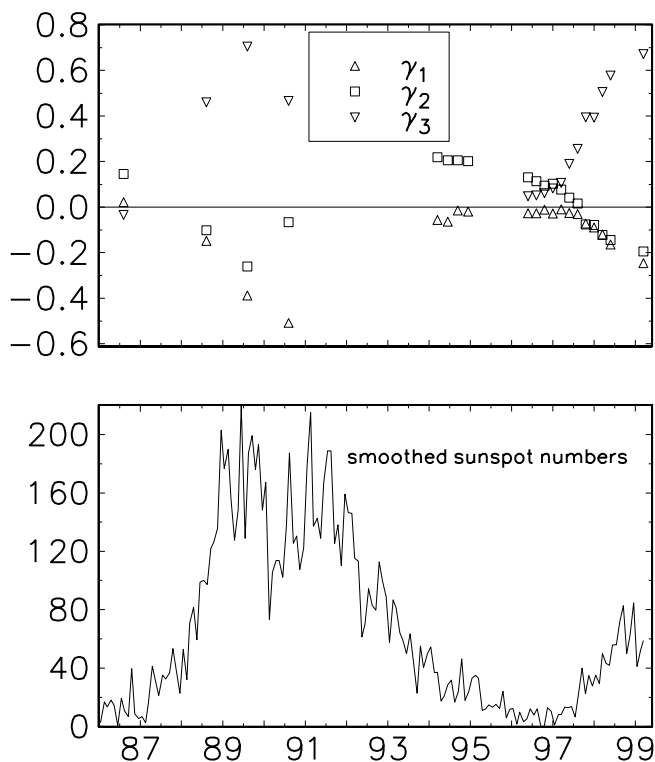


FIG. 6.—*Lower panel*: Monthly averages of the sunspot number covering the period from 1986 through early 1999. *Upper panel*: Mean γ 's covering from 1986 through early 1999. The first cluster of points is from BBSO data (1986–1990). The second is from LOWL data (1994), and the third is from MDI data.

1998 and early-1999 MDI measures of activity were midway between their counterparts from the last cycle for the years 1988 and 1989—except for γ_0 , which is slightly weaker in 1998 than it was in 1988.

Furthermore, in Figure 5 we show the principle result of this section obtained from the γ 's of 1998.4. The frequency dependence in $\Delta\nu$ primarily reflects mode inertia. Two points are worth emphasizing. The first is that for full-disk measurements, the anticipated frequency change in these measurements should be weakly l dependent. This is so because the unresolved peaks in $l=2$ are dominated by their $m = \pm 2$ components (over $m = 0$) and, similarly, in $l=3$ are dominated by their $m = \pm 3$ components (over $m = 1$). The second point is that the complete $l=2$ and 3 multiplets would be visibly asymmetric for high frequencies. As for the scale of the change, the reader should bear in mind that the rotational splitting between adjacent peaks is about $0.45 \mu\text{Hz}$.

4. CONNECTION TO OTHER CHARACTERISTICS OF SOLAR ACTIVITY

The close link between the even a -coefficients and the Sun's latitudinal thermal structure (Kuhn, Libbrecht, & Dicke 1988) has been demonstrated by Kuhn (1988, 1998), Libbrecht & Woodard (1990), and Woodard & Libbrecht (1991).

Bachmann & Brown (1993) demonstrated a strong correlation among the centroid shifts and various characteristics of activity, including the Mg II 280 nm core-to-wing ratio, the 10.7 cm radio flux, the He I 10830 Å index, the Kitt Peak magnetic index, the EUV flux, and the Magnetic Plage

Index Strength. A similar analysis for the new cycle based on GONG data has been presented by Bhatnagar et al. (1999), in which they find a strong correlation to most of the characteristic indices of activity. They used essentially the same indices as Bachmann & Brown. A similar result was obtained from GONG data by Howe et al. (1999), but their results extend over a longer time interval. They also analyzed the behavior of the splitting coefficients (to P_6). Perhaps their most significant find is a clean correlation between the even a -coefficients and the corresponding Legendre coefficients of a fit to the Kitt Peak magnetograms. We report here a similar result based on the BBSO Ca K plage data, but to a higher Legendre order.

First however, we show in Figure 6 the temporal evolution of the γ 's over 13 years. This figure is an extension of Figure 4 of Dziembowski et al. (1998). The extension is the inclusion of seven more 72 day long MDI sets and the inclusion of the corresponding smoothed sunspot numbers. The mean values of the γ -coefficients are from various sources, including BBSO, LOWL, and *SOHO*/MDI. The BBSO data are from Woodard & Libbrecht (1991), and LOWL data are from S. Tomczyk (1996, private communication). We compare the γ 's with the monthly averages of smoothed sunspot numbers. Clearly, the BBSO data of 1988 and 1989 give the largest magnitudes of the γ 's, and this corresponds to the first half of the previous sunspot maximum. Unfortunately, we are missing splitting data from the rising phase (1987 or so) as well as from the declining phase of the solar cycle. The errors in the BBSO and LOWL γ 's are about twice as large as those in *SOHO*/MDI, but they are still relatively small and would not be visible in Figure 6.

For the current rising cycle, the rapid rise, especially of P_6 , coincides with the rise of the sunspot number. Based on a comparison with the previous maximum, it can be noted that the maximum value of γ_3 (at 1999.2) corresponds to a much higher activity level than is reflected in the sunspot number. The difference can be only partially explained by the difference in mode sets used to infer the γ in the BBSO and MDI sets. There is some sensitivity of the inferred γ 's to the maximum l in the set. The maximum l in the MDI sets is between 197 and 200, while that in the BBSO sets is 140. We find that by truncating the MDI data, we get absolute values that are a few percent lower (typically 1%–3%).

In Figure 7, we show a series of Legendre decompositions of successive quarterly averages of daily BBSO Ca II K images using one image per day. We also show the corresponding γ 's from the MDI data. In Figure 7, we show the P_2 -, P_4 -, and P_6 -coefficients of that decomposition. We do not show the $k=0$ term because of problems in absolute calibration. In Figure 7, there is a systematic correlation between the β 's of the quarterly Ca K data and the corresponding γ 's. The strongest correlation is between the P_6 terms. The correlation coefficient is 0.95 and is somewhat larger than that for P_2 . The correlation for P_4 is 0.6. This relatively lower value reflects the tendency of γ_2 to continue to increase in the most recent data, while β_2 has begun to decrease. The close agreement between the β 's and γ 's continues through P_{10} , as can be seen in Figure 8. For P_8 and P_{10} , the correlation is about 0.8, but sharply falls to 0.2 for the P_{12} term. The breakdown in the agreement comes for γ_6 because it lacks the clear trend evident in the lower ranking terms. Still, it is impressive that there is such a strong correlation in the temporal evolution, from P_2 through P_{10} ,

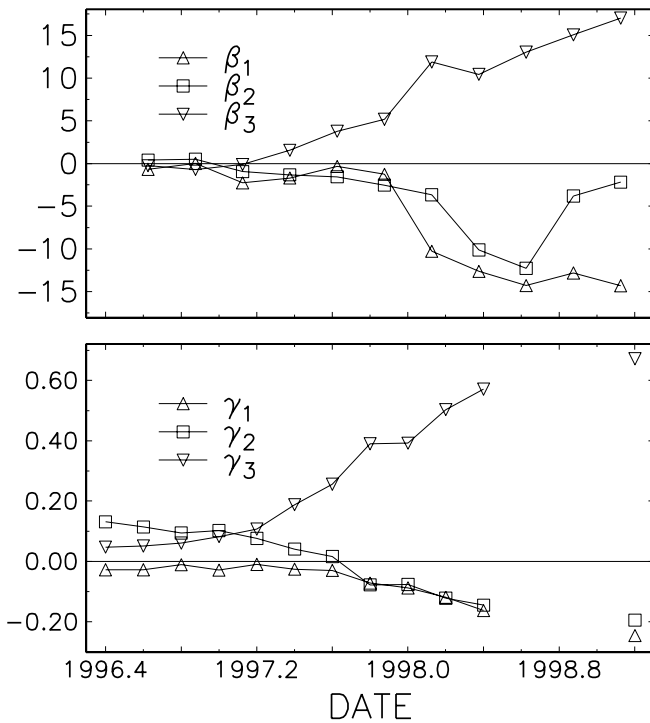


FIG. 7.—Upper panel: Quarterly P_2 , P_4 , and P_6 distortions in the BBSO Ca II K data. This is to be compared to the corresponding γ 's from the MDI data. The β 's are from a Legendre fit, and the ordinate is in arbitrary units. The error bars are within the symbols.

between a measure of the magnetic field and the asymmetries in the oscillation multiplets.

Another feature to notice in Figure 7 is that the P_4 asymmetry (β_2) in the years of solar minimum is much less visible

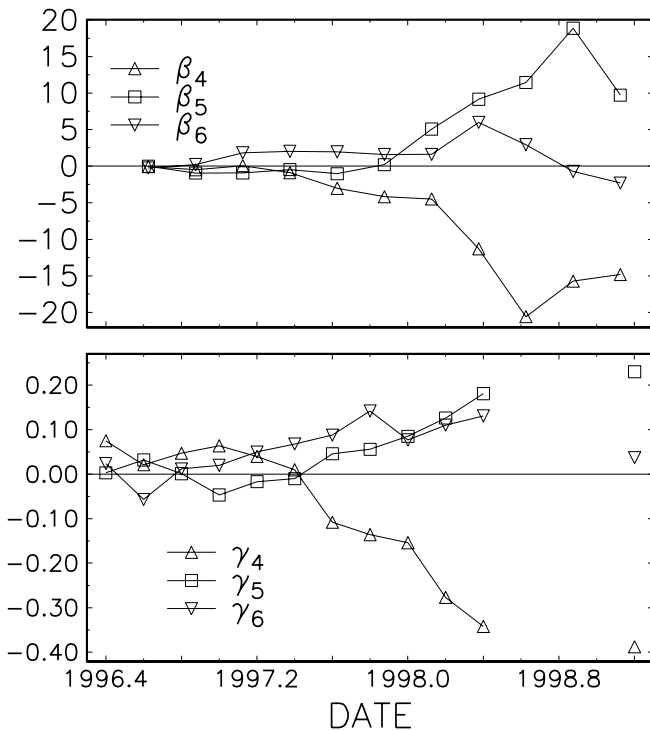


FIG. 8.—Upper panel: Quarterly P_8 , P_{10} , and P_{12} distortions in the BBSO Ca II K data (in arbitrary units). This is to be compared to the corresponding γ 's from the MDI data. The error bars are within the symbols.

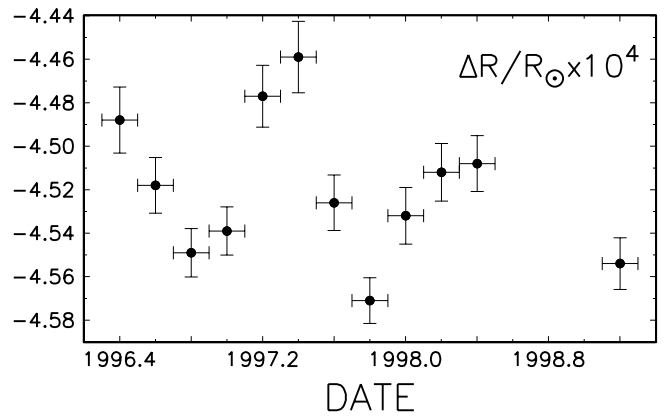


FIG. 9.—Relative differences in the radius of the Sun, multiplied by 10^4 , inferred from f -mode frequencies and the standard solar model (Christensen-Dalsgaard et al. 1996).

than the corresponding helioseismic asymmetry expressed by γ_2 . Is this evidence of a distinct origin of γ_2 ?

While we see the same trends in the β 's and γ 's in Figures 7 and 8, we also see some differences. For instance, the ratio of γ_3 to γ_1 or γ_2 is about 3 times the value of its β counterpart. The reversal of the decreasing trend in the β_2 -coefficient does not have its counterpart in the behavior of γ_2 . However, based on the behavior of γ_2 during the previous cycle (see Fig. 6) we may expect that such a reversal should happen soon.

5. CHANGES IN THE SOLAR RADIUS

Spruit (1998) says that “if variations in $\Delta R/R$ much exceeding a few times 10^{-7} were reliably detected, the implications would be much more serious than a mere contradiction between, say, a dynamo theory and observations of the solar cycle.” The changes in the radius inferred from fundamental mode frequencies reported by Dziembowski et al. (1998) exceed this by 1 order of magnitude.

In Figure 9, we show the results of radius variations now extended to include the full 12 sets of MDI f -mode data available. Here the amplitude of the changes is even larger than we reported earlier for the first five data sets. However, there is no systematic trend correlated with sunspot numbers. We cannot offer any explanation for the observational results, and we warn readers against interpreting the results too literally, because the relation between the true radius and that inferred from f -modes is not clear because there may be instrumental sources for f -mode frequencies at the 10^{-5} level.

We note that the lack of a trend is in sharp contrast with the behavior of the Sun's spherical symmetry as reflected in γ_0 over the same interval shown in Figure 1.

6. SEARCH FOR AN INTERIOR SIGNATURE OF SOLAR CYCLE VARIABILITY

The main advantage of a helioseismic probing of solar variability over the cycle is the prospect of detecting changes beneath the photosphere. There is strong evidence that most of the signal we see in the γ 's arises close to the surface. Of course, it would be important to know exactly how close and whether or not we can see a signal from deeper layers.

The problem of localizing the perturbation cannot be completely separated from its physical cause. Goldreich et al. (1991) derived a formula connecting p -mode frequency changes to changes in entropy and magnetic field intensity. They used their formalism to assess the required field intensity and infer the localization of the perturbation needed to explain the changes in centroid frequencies. They concluded that the main contribution arises from the photospheric region, while there is significant contribution from much higher layers for high-frequency modes. The latter conclusion is based on the observation that there is a sharp drop in $\Delta\nu$ at very high frequencies (above 3.5 mHz). We stress that we do not find such an effect in the *SOHO* data. There is some saturation in the growth of $\Delta\nu$ at high frequencies. This is primarily a property of mode inertia. After an initially sharp decrease with ν , the inertia reaches its maximum at about 3.5 mHz and then slowly declines. The intrinsic behavior of the spherically symmetric part of the perturbation is best revealed in γ_0 , shown in Figure 4. Here one observes an increase rather than a decrease in γ_0 above 3.0 mHz. The weak dependence of γ_0 on frequency (the same holds for the other γ 's) points to a localization of the perturbation close to the photosphere, where we normalize our eigenfunctions for evaluating mode inertia. Unfortunately, not much more can be inferred from the weak frequency dependence of the γ 's.

The observational evidence strongly supports the view that, more or less, there is a direct role of the magnetic field in producing the frequency changes. The formalism of Goldreich et al., in principle, describes radial pulsation. However, it may be applied to all modes, if the perturbation is localized well above the modes' lower turning point. This restriction is a clear shortcoming of the formalism when applied near the surface because helioseismic diagnosis rests primarily on differential sampling, which depends mostly on l .

With this in mind, we developed a formulation which is free from the aforementioned shortcomings. In particular, we developed formulae connecting the magnetic field and the resulting perturbation of the thermodynamical quantities and their combined effect on the oscillation frequencies. Furthermore, we considered the θ dependence of the mean magnetic field, which enabled us to develop corresponding connection formulae for the even a -coefficients.

We focus our attention on the case of an isotropic, random field. Specifically, we set

$$\overline{B_i B_j} = \frac{B^2(r, \theta)}{3} \delta_{ij}, \quad (5)$$

where the quantities in the formula have their usual meanings. Then, we represent B^2 in the form

$$B^2(r, \theta) = 24\pi \sum h_k(r) P_{2k}(\cos \theta). \quad (6)$$

Of course, there may exist an antisymmetric component with respect to the equator, but in a linear treatment of the perturbation of the magnetic field, such effects do not contribute. Mechanical equilibrium implies

$$\frac{d}{dr} (p_k + h_k) = -\rho_k g - \rho \frac{d\phi_k}{dr}, \quad (7)$$

$$p_k + h_k = -\rho\phi_k \quad \text{for } 2k > 0, \quad (8)$$

where the subscript k denotes the corresponding coefficient of the expansion of the respective quantities.

Note that equations (7) and (8) imply that

$$\phi_k \equiv \rho_k \equiv 0, \quad (9)$$

$$\frac{u_k}{u} = \frac{p_k}{p} = -\frac{h_k}{p}, \quad (10)$$

where $u = P/\rho$. Except for the ionization zones, we have $u_k/u \approx T_k/T$.

In the adopted approximation, the magnetic field just acts like an additional pressure. It is well known that as long as such a pressure is isotropic, it does not disrupt the star's spherical symmetry, insofar as the dynamical parameters are concerned.

Equation (10) implies that zones with stronger fields should be cooler. Of course, in order to maintain thermal balance, an aspherical component must be present in the convective flows—a close analog to the classical meridional circulation in rigidly rotating stars. Here we assume that the effects of such flows may be ignored in equations (7) and (8).

There are important physical distinctions resulting from the differences between the spherical and nonspherical parts of the perturbation. For the spherical part, the connection between h_k and the corresponding thermodynamical parameters requires that one consider the star's thermal balance. For the nonspherical part, mechanical equilibrium conditions alone suffice. For the inversion formalism, this means that for the spherically symmetric perturbation we have to consider two unknown structural functions, u_0 and h_0 . We identify these two unknown functions with the differences between the current and the solar minimum values of u and h . Thus, we set

$$\Delta u \equiv u_0, \quad \Delta h \equiv h_0.$$

In the Appendix we derive the following connection formula:

$$\Delta \bar{\nu} = \nu \int_0^1 \left(\mathcal{K}_u \frac{u_0}{u} + \mathcal{K}_h \frac{h}{p} \right) d\tau, \quad (11)$$

where τ is the acoustic radius,

$$\tau = \int_0^r \frac{dr'}{c} \left(\int_0^R \frac{dr'}{c} \right)^{-1}.$$

The explicit forms of \mathcal{K}_u and \mathcal{K}_h are given in equations (A19) and (A20) of the Appendix.

On the other hand, for the splitting coefficients that reflect the nonspherically symmetrical part, we make an approximation. The approximation here is that we ignore one term that can be appreciable only near the lower turning point. This term mixes the h_k term with its counterparts of lower rank. This term arises from the modification of the Lorentz force by the oscillations. In our preliminary analysis here, we use this approximation as well as equation (10) to express h_k in terms of u_k . In this way, as shown in the Appendix, we obtain

$$a_{2k} \cong C_{k,s} \nu \int \mathcal{K}_{u;a} \frac{u_k}{u} d\tau. \quad (12)$$

The explicit form of the kernel is given in equation (A18). Potentially significant contributors to the time-dependent perturbation are the Reynolds stresses. We do not consider them here, but plan to address their role in a future work.

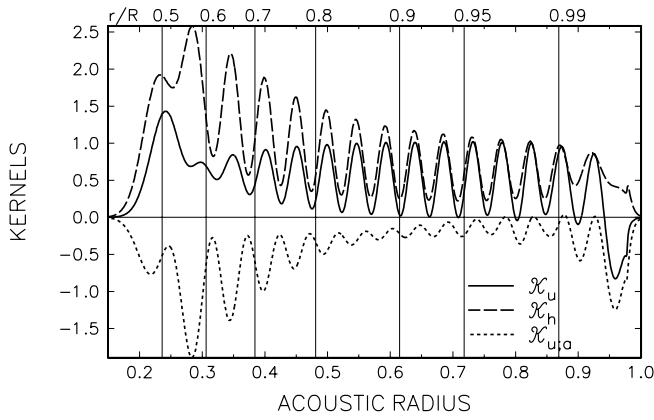


FIG. 10.—Kernels $K_{u,0}$, K_h , and $K_u^{(a)}$ vs. the acoustic radius and fractional radius.

Our sole aim here is to search for any signature of changes in the interior.

In Figure 10, we show examples of the three kernels in equations (11) and (12) for $l = 20$, $\nu = 3$ mHz, and $n = 15$. It is important to notice that throughout most of the interior, the two kernels K_u and K_h are very similar. This sends a rather grim message about the prospect of disentangling the magnetic field and temperature perturbations.

6.1. Inversion for Spherically Symmetric Changes

Because of the similarity between the two kernels, K_u and K_h , we did not attempt to solve a simultaneous inversion problem. Rather, we solved separate inverse problems, ignoring, respectively, the u_0 and h_0 contributions. We used an optimal averaging method (SOLA, developed by Pijpers & Thompson 1994).

In Figure 11, we see how various treatments of the near-surface cycle-dependent perturbation affect the inversion for the temperature difference. Removing γ_0/I from the measured $\Delta\nu/\nu$ values amounts to subtracting the unresolved, near-surface contribution that apparently makes up most of the values of $\Delta\nu/\nu$. We see that there is a cross talk problem. However, there is a common feature, and that is the rise of $\Delta u/u$ between 0.5 and 0.7 of the acoustic radius. Furthermore, the differences among the results obtained with various $N_\gamma > 0$ are less than the 1σ errors shown in

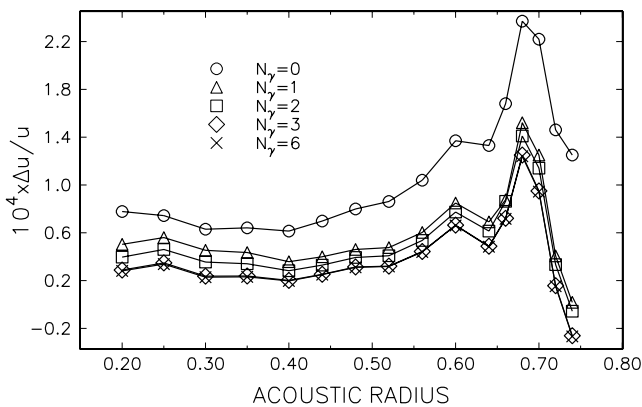


FIG. 11.—Result of inversions of the frequency differences for the relative temperature perturbation between 1999.2 and 1996.4. N_γ denotes the number of terms in the polynomial representation of $\gamma_0(\nu)$; $N_\gamma = 0$ means that effects of the near-surface perturbation have not been removed.

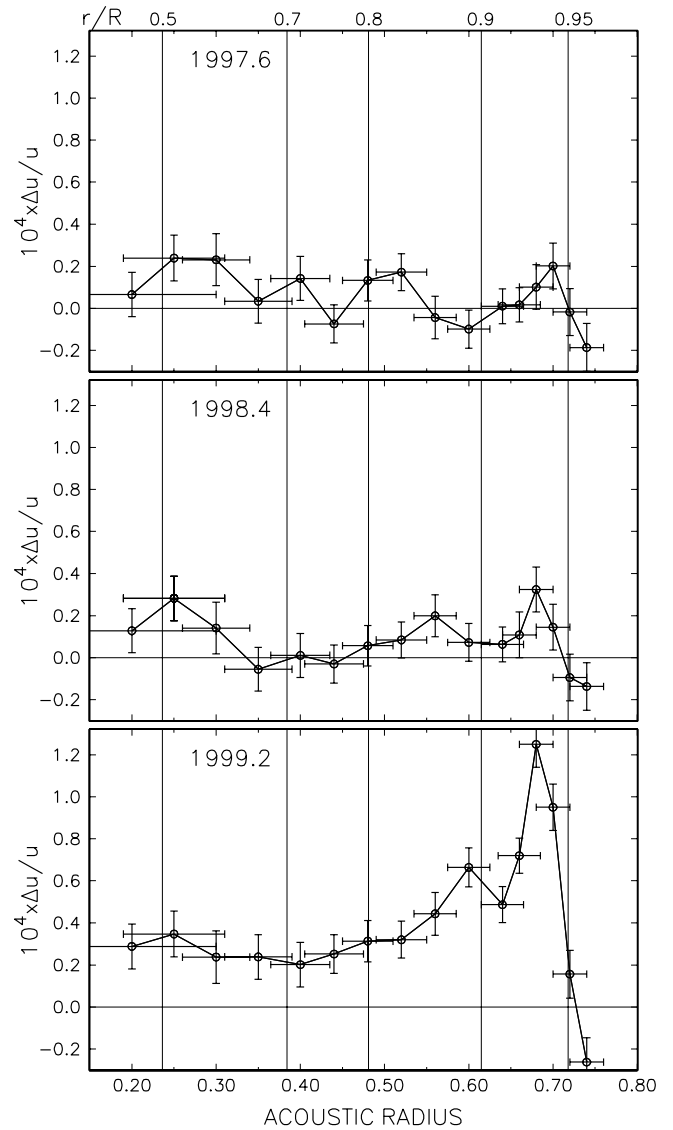


FIG. 12.—Inversions of the frequency differences between indicated years and 1996.4 with the near-surface contribution eliminated.

Figure 12. The γ_0 terms used to obtain the results shown in Figure 12 were obtained with a three-term polynomial representation of the $\gamma(\nu)$ dependence, as shown in Figure 4. The fact is, however, the results are insensitive to the number of terms in the polynomial—a constant γ gives a similar result. What this means to us is that the contribution to $\Delta\nu/\nu$ seen in Figure 11 cannot be eradicated by a judicious adjustment of the near-surface contribution.

We believe that removing γ_0 is more realistic than leaving it in. There are many uncertainties in modeling the outermost part of the Sun (see Kosovichev 1995 for a recent discussion), and there are various possible sources of frequency changes arising there that are difficult to disentangle. In all subsequent analysis, we remove the near-surface effect by subtracting a three-term representation of $\gamma(\nu)$. Still, there is a good part of the Sun's interior where, even with the data we have in hand, one could not build a satisfactory kernel. In the three panels of Figure 12, we show the temporal evolution of the perturbation with respect to 1996.4, the time of activity minimum. The most significant result from all of our inversions is the increase in

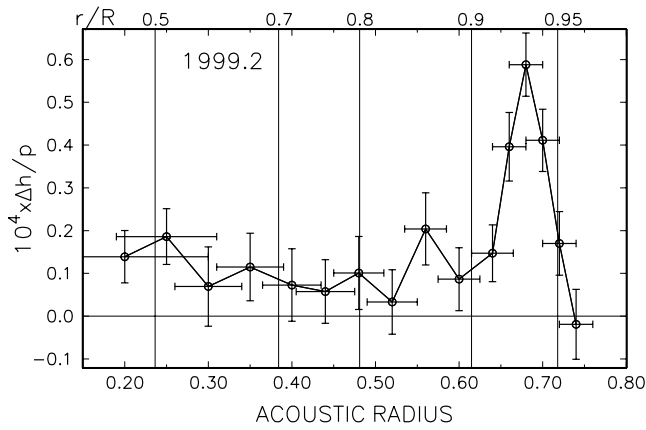


FIG. 13.—Inversion of the frequency differences between 1999.2 and 1996.4 to determine the magnetic field changes with the near-surface contribution removed.

$\Delta u/u$ between 0.4 and 0.68 (where it peaks) of the acoustic radius; at the peak, we find a value which exceeds the errors by a factor of 10. We also see peaks at the same location in the inversion of earlier data sets, but of much lower amplitude.

If indeed the peak at 0.68 were mostly due to a temperature perturbation, then the $\Delta u/u$ value of $\approx 1.2 \times 10^{-4}$ inferred from the last data sets means a 400 K temperature perturbation at a depth of 45 Mm.

In Figure 13, we show the results of inversions for Δh with Δu set to zero. There are differences in the details as compared with Figure 12; however, the peak at 0.68 remains. The value of Δh at the peak (6×10^{-5}) implies a $\langle B^2 \rangle$ of $(60 \text{KG})^2$, which is at the lower limit of the current best guess of that quantity at the base of the convection zone (D’Silva & Choudhuri 1993; D’Silva & Howard 1993); however, it is far greater than the current estimates of $\langle B^2 \rangle$ on the Sun’s surface, about $(0.07 \text{KG})^2$ (Kuhn 1998).

Perhaps the peak at 0.68 is an artifact of the data analysis. However, one argument in its favor comes from the fact that Howe et al. see the same peak. They inverted the frequency differences using the GONG data. They performed a regu-

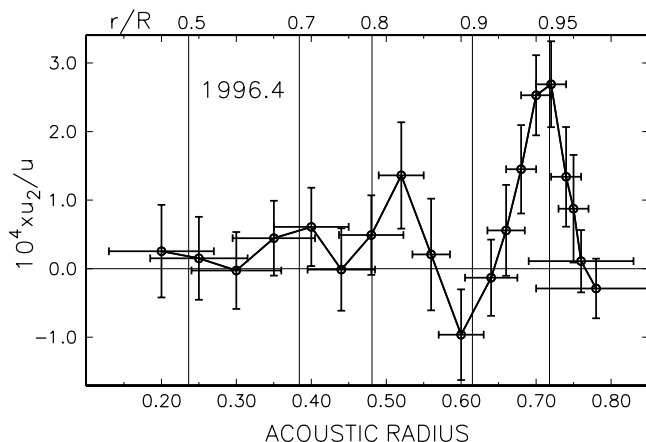


FIG. 14.—Inversion of the a_4 splitting coefficients for the P_4 temperature perturbation at activity minimum.

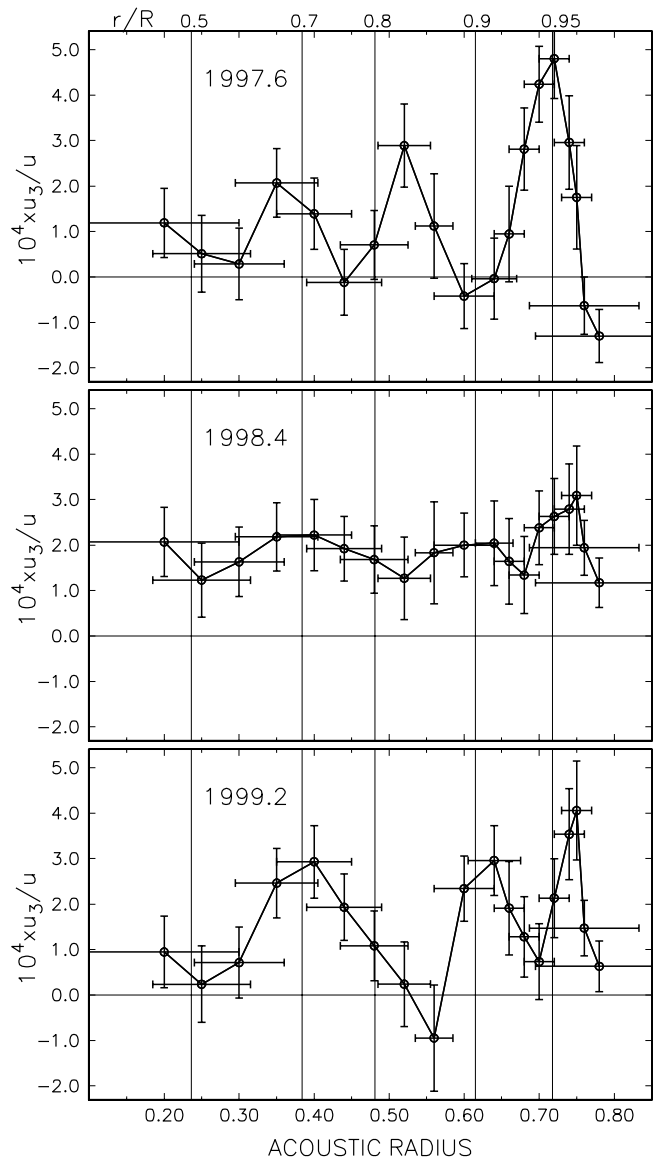


FIG. 15.—Inversion of the a_6 splitting coefficients for the relative P_6 temperature perturbation from three time periods.

larized least-squares inversion, which makes it difficult to fully believe the features they calculate. In fact, they did not regard the feature of interest here as being significant. Nonetheless, when we look at their Figure 6, we notice that they also find a peak near the same point that we do.

6.2. Inversion for Angular Structure

We look for the signature of the interior by inverting the a -coefficients for which the signal is the strongest.

As in the inversions for radial structure, we remove the appropriate γ_k -coefficient from a_{2k} in equation (12). Explicitly, we remove the contribution of $C_{k,l} \gamma_k(\nu) / I_{n,l}$ to a_{2k} .

We begin our analysis with the a_4 -coefficients from 1996.4. Throughout the solar minimum, the a_4 -coefficients were the only appreciable oscillation coefficients describing solar asymmetry. The result of our inversion for 1996.4 is shown in Figure 14. The feature of interest here is the sharp rise in the relative temperature in the interval between 0.60

and 0.70, which is closer to the surface than the peak in the inversions for radial structure. The result has a 4σ significance. Note that the maximum value of u_2/u is about twice as large as the maximum value of $\Delta u_0/u$ seen in Figure 12. The values of the corresponding γ 's (see Fig. 1) are similar. The positive values of u_2 imply negative values of the magnetic field coefficient of equation (6). That is, a higher temperature implies a lower magnetic field.

We remark that inversions of a_4 's of subsequent data sets fail to reveal any persistent temporal trend—in contrast to what we have seen in the behavior of γ_2 . The only persistent feature is the peak at acoustic radius $\tau \approx 0.72$.

In Figure 15, we show the results of inversions of a_6 —the dominant terms in the years of higher activity (see Fig. 1). We selected three data sets from the phase of high activity.

As in the previous case, the peak is in shallower layers (at 0.76 in acoustic radius, or a depth of 24 Mm). The maximum value of u_6/u is even larger than the maximum value of u_4/u . The results are marginally significant at a 3σ level. The plots illustrate a lack of any temporal trend. Thus, we attach less weight to them than to the results from the inversions for the radial structure.

We should stress, however, that a sound speed perturbation of a similar size and localization has been seen before. Kosovichev (1996) found it from an inversion of time-distance data taken in 1991—that is, during the previous solar maximum. Finally, we point out that Kosovichev (1999) has found evidence for a statistically significant perturbation near the base of the convection zone from GONG data taken during the current rising phase of activity.

7. CONCLUSIONS

We find a rapid rise in the seismic signature of solar activity between 1997.5 and 1998.4 (the end of the MDI data set). The signatures are the even a -coefficients describing asymmetries in oscillation multiplets. For the first time, we were able to determine significant asymmetries extending up to P_{18} . We compared the temporal and angular asymmetries of the Sun from oscillations from *SOHO*/MDI with BBSO Ca II K data. We found clear temporal and angular correlations, through P_{10} , between the two extending over the rising phase to date. The comparison indicates a direct link between changes in the surface magnetic field and solar oscillation frequencies.

We also examined changes in the Sun's radial structure implied by the changes in centroid frequencies of oscillation multiplets. The typical frequency change at 3 mHz was about $0.1\ \mu\text{Hz}$ over the interval considered.

We used information about the Sun's asymmetries and radial structure changes to predict the multiplet structure for low-degree modes for spatially unresolved observations. Furthermore, we showed that there should be a significant asymmetry in the full multiplet structure for low values of l .

We used data on f -modes to infer information about changes in the Sun's seismic radius. We found relative changes on the order of 10^{-5} , but without a visible trend.

We searched for a signature of solar cycle changes in the Sun's interior by means of optimally averaged inversions of the frequency differences and the splitting coefficients. We believe that we obtained a significant result from the former analysis. We found the most significant change in the layer located at a depth ranging between 25 and 100 Mm with a peak at 45 Mm. The perturbation may be due to a relative temperature increase peaking at 12×10^{-5} or an increase in $\langle B^2 \rangle$ peaking at $(60\text{KG})^2$ (or some combination thereof). We are unable to disentangle the two.

We can only speculate about the nature of this perturbation. Since the implied field intensity is significantly stronger than that on the Sun's surface, this may indicate a role of convective downdrafts in preventing the field from reaching the photospheric layers.

The inversion of the splitting coefficients reveals, in principle, the angular structure of the perturbation and yields less significant results. The maximal value of the perturbation occurs in the outermost layers, peaking at a depth of about 30 Mm beneath the surface. Presumably, such a field would be dissipated in situ.

This is a preliminary work. We plan several interrelated projects for the future. (1) We will follow changes in the γ 's during the current rising phase of activity and subsequently through the maximum and declining phase of Cycle 23. After all, we lack corresponding information from Cycle 22. (2) We will invert even a -coefficients from data with higher l -values to improve the spatial resolution in the outer layers. (3) We will study intensity bands in various wavelengths to get information on the vertical distribution of the temperature perturbation. (4) We will develop the connection formulae linking frequency changes to temperature, magnetic fields, and velocity fields assuming various models of the random fields. (5) We will consider the energy balance in the outer layers, taking into account the effects of field dissipation, as well as the modification of the convective transport by the field. This is essential because there is no unique interpretation of the values of $\Delta\nu$ and the even a -coefficients, so that ultimately the interpretation requires physical models that must be compared with data through a forward problem. Furthermore, this is needed to link luminosity and irradiance variations. The requisite information about luminosity is in the values of $\Delta\nu$, but we need models to decode it.

SOHO is a project of international cooperation between ESA and NASA. This research was supported by the SOI-MDI NASA contract NAG 5-3077 at Stanford University and partially supported by NSF ATM-97-14796 and NASA NAG5-4919 grants to Big Bear and KBN-2-P03D-014-14 to W. A. D.

APPENDIX

Our starting point in the derivation of equations (11) and (12) is the perturbed equation for adiabatic oscillations,

$$\omega^2 \rho \xi = \mathcal{F}(\xi). \quad (\text{A1})$$

We consider a Eulerian (Δ) perturbation of \mathcal{F} arising from the action of the isotropic magnetic field, described by equations (5) and (6). The associated frequency perturbation $\Delta\omega$ may be evaluated with the use of the variational principle defined by equation (A1) (e.g., Unno et al. 1989). In this way, we get

$$\frac{\Delta v}{v} = \frac{\Delta\omega}{\omega} = \frac{1}{2\omega^2 I} \int d^3x [\xi^* \cdot \Delta\mathcal{F}(\xi) - \Delta\rho\omega^2 |\xi|^2], \tag{A2}$$

where ξ is the displacement eigenvector calculated in an unperturbed spherically symmetric solar model and

$$I = \int d^3x \rho |\xi|^2. \tag{A3}$$

The expression is applicable for any mode. We will not use the l and n subscripts unless it is necessary.

The eigenvectors are used in the standard form

$$\xi = r[y(r)e_r + z(r)\nabla_H]Y_l^m(\theta, \phi) \exp(-i\omega t), \tag{A4}$$

where y and z are radial eigenfunctions determined for each mode together with unperturbed ω . We will also use eigenfunction q defined through the expression

$$\nabla \cdot \xi = q(r)Y_l^m(\theta, \phi) \exp(-i\omega t). \tag{A5}$$

We now split $\Delta\mathcal{F}$ into the part resulting from the distortion of the structure, $\Delta_D\mathcal{F}$, and the part resulting directly from the Lorentz force, $\Delta\mathcal{F}_L$. With the Cowling approximation, which is well justified in our case, we have for the first part

$$\Delta_D\mathcal{F} = -\nabla[\Delta(p\Gamma_1)\nabla \cdot \xi + \xi \cdot \nabla(\Delta p)] - g e_r \cdot \nabla(\Delta\rho\xi), \tag{A6}$$

where Γ_1 is the adiabatic exponent and g is the gravitational acceleration, and for the second part we have

$$\Delta\mathcal{F}_L = \frac{\mathbf{b} \times (\nabla \times \mathbf{B}) + \mathbf{B} \times (\nabla \times \mathbf{b})}{4\pi}, \tag{A7a}$$

where

$$\mathbf{b} = \nabla \times (\xi \times \mathbf{B}). \tag{A7b}$$

The contributions from the two parts are calculated separately.

Let us consider first the frequency change, $\Delta_D v$, resulting from $\Delta_D\mathcal{F}$ and $\Delta\rho$. The perturbed parameters are represented, as explained in § 6, as a series of Legendre polynomials of even order. These series and representations of ξ given in equations (A5) and (A6) are used in equation (A2). After integration over spherical surfaces and certain integrations by parts over r , we get

$$\frac{\Delta_D v}{v} = \sum_k \kappa_{kl}^m \int_0^R \left(\tilde{\mathcal{K}}_u \frac{u_k}{u} + \mathcal{K}_p \frac{p_k}{p} + \mathcal{K}_d \frac{r}{p} \frac{dh_k}{dr} \right) dr. \tag{A8}$$

The boundary terms at $r = R$ are neglected because they contribute only to the γ_k -coefficients, which are treated separately. The kernels, $\tilde{\mathcal{K}}_u$, \mathcal{K}_p , and \mathcal{K}_d , are calculated in the approximation applicable to solar p -modes, that is, to leading order in the three parameters

$$l, \quad V = \frac{gr\rho}{p}, \quad s = \omega \sqrt{\frac{r}{g}},$$

which may be large. The corresponding scaling of the eigenfunctions is $zl \sim y$ and $q \sim s^2 y$ in the outer evanescent zone and $q \sim s\sqrt{V}y$ in the acoustic propagation zone. Keeping only the leading-order terms, we have

$$\tilde{\mathcal{K}}_u = \left\{ y^2 + \Lambda z^2 - \frac{1}{s^2} \left[\Gamma_1 qy + 2\Lambda yz + \frac{q^2}{V} \left(\frac{\partial \Gamma_1}{\partial \ln \rho} \right)_p \right] \right\} \frac{\rho r^4}{2I}, \tag{A9}$$

$$\mathcal{K}_p = \frac{q^2}{s^2 V} \left[\left(\frac{\partial \Gamma_1}{\partial \ln \rho} \right)_p + \left(\frac{\partial \Gamma_1}{\partial \ln p} \right)_\rho \right] \frac{\rho r^4}{2I}, \tag{A10}$$

$$\mathcal{K}_d = \frac{qy}{s^2} (\Gamma_1 - 1) \frac{\rho r^4}{2I}, \tag{A11}$$

where $\Lambda = l(l + 1)$.

Now we consider the remaining part of the relative frequency change, which is

$$\frac{\Delta_L v}{v} = \frac{1}{2\omega^2 I} \int d^3x \xi^* \cdot \Delta\mathcal{F}_L(\xi). \tag{A12}$$

It is more convenient to work with the Cartesian vector components. Then, from equation (A7a) we have

$$-(\Delta \mathcal{F}_L)_k = \frac{1}{4\pi} (b_j B_k + B_j b_k - \delta_{jk} \mathbf{B} \cdot \mathbf{b})_{,j} \equiv T_{jk,j}, \tag{A13}$$

and from equation (A8) we have

$$b_k = B_n \xi_{k,n} - \xi_n B_{k,n} - B_k q.$$

Thus, using equation (5), we obtain

$$T_{jk} = \left(\xi_{j,k} + \xi_{k,j} + \frac{q^2}{2} \delta_{jk} \boldsymbol{\xi} \cdot \nabla \right) \frac{B^2}{12\pi},$$

which with the use of equation (6) allows the expression of $\Delta \mathcal{F}_L$ in terms of h_k and their derivatives. After integration by parts in equation (A12), we get, keeping again only to the leading-order terms,

$$\frac{\Delta_L v}{v} = \frac{1}{2\omega^2 I} \sum_k \left[\kappa_{kl}^m \int_0^R \left(\mathcal{J} h_k + qyr \frac{dh_k}{dr} \right) r^2 dr + 2\alpha_{kl}^m \int_0^R z^2 h_k r^2 dr \right], \tag{A14}$$

where

$$\mathcal{J} = 2q^2 + 2\Lambda \left[2y + \left(\frac{d \ln \rho}{d \ln p} \Gamma_1 - 1 \right) \frac{gq}{s^2} \right]^2, \tag{A15}$$

$$\alpha_{kl}^m = \int P_{2k} \left| \frac{\partial^2 Y_l^m}{\partial \theta \partial \phi} \right|^2 \sin \theta d\theta d\phi. \tag{A16}$$

The second term in equation (A14), which formally is of the leading order, is neglected in our calculations. This term involves the angular integrals that are not reduced to single coefficients, κ_{kl}^m . It may be expressed in terms of all coefficients of orders $\leq k$, which implies that each k -component in the representation of the magnetic field given in equation (6) contributes to all a_{2j} -coefficients with $j \leq k$. We checked numerically that the contribution to the kernels arising from this term is small. With this additional simplification, there is a one-to-one correspondence between the a_{2k} - and h_k -coefficients and the kernels do not depend on k .

Combining equations (A8) and (A15) we get, after integrating parts to eliminate the derivative of h_k ,

$$\frac{\Delta v}{v} = \sum_k \kappa_{k,l}^m \int_0^R \left(\mathcal{K}_p \frac{p_k}{p} + \tilde{\mathcal{K}}_u \frac{u_k}{u} + \tilde{\mathcal{K}}_h \frac{h_k}{p} \right) dr, \tag{A17}$$

where

$$\tilde{\mathcal{K}}_h = \left\{ y^2 + \Lambda z^2 + \frac{1}{s^2} \left[\frac{\mathcal{J} - q^2 \Gamma_1}{V} - qy \left(1 - \frac{\Lambda}{Vs^2} \right) + \Lambda yz \right] \right\} \frac{\rho r^4}{2I}.$$

For $k > 0$, we make use of equation (10) in equation (A17). Then, changing the integration variable to τ , as used in equation (11), we get

$$\Delta v_k = \kappa_{k,l}^m v \int_0^1 \mathcal{K}_{u;a} \frac{u_k}{u} d\tau,$$

with

$$\mathcal{K}_{u;a} = v c (\tilde{\mathcal{K}}_u + \mathcal{K}_p - \tilde{\mathcal{K}}_h) \int_0^R \frac{dr}{c}. \tag{A18}$$

The kernels $\tilde{\mathcal{K}}_u$ and $\tilde{\mathcal{K}}_h$ are given in equations (A9) and (A18), respectively. Equation (12) follows immediately from equations (2) and (A18).

In the case of $k = 0$, we first consider the integral

$$J_p = \int_0^R \mathcal{K}_p \frac{p_k}{p} dr$$

and define

$$\frac{dM_p}{dr} \equiv K_k.$$

After integration by parts, we get

$$J_p = \frac{p_0}{p} \mathcal{M}_p \Big|_0^R - \int_0^R \mathcal{M}_p \frac{d}{dr} \left(\frac{p_0}{p} \right) dr.$$

We use equation (7), with ϕ_0 neglected, to eliminate the derivative of p_0 and once more integrate by parts to eliminate the derivative of h_0 . In this way, ignoring the boundary terms, we obtain

$$J_p = - \int_0^R \left[\mathcal{K}_p \frac{h_0}{p} + \frac{\mathcal{M}_p V}{r} \left(\frac{u_0}{u} + \frac{h_0}{p} \right) \right] dr .$$

With this result, we get from equation (A17)

$$\Delta \bar{v} = v \int_0^1 \left(\mathcal{K}_u \frac{u_0}{u} + \mathcal{K}_h \frac{h_0}{p} \right) d\tau ,$$

where

$$\mathcal{K}_u = c \left(\tilde{\mathcal{K}}_u - \frac{\mathcal{M}_p V}{r} \right) \int_0^R \frac{dr}{c} , \quad (\text{A19})$$

$$\mathcal{K}_h = c \left(\tilde{\mathcal{K}}_h - \mathcal{K}_p - \frac{\mathcal{M}_p V}{r} \right) \int_0^R \frac{dr}{c} . \quad (\text{A20})$$

REFERENCES

- Bachmann, K. T., & Brown, T. M. 1993, *ApJ*, 411, L45
 Bhatnagar, A., Jain, K., & Tripathy, S. C. 1999, *ApJ*, 521, 885
 Christensen-Dalsgaard, J., et al. 1996, *Science*, 272, 1286
 D'Silva, S., & Choudhuri, A. R. 1993, *A&A*, 272, 621
 D'Silva, S., & Howard, R. F. 1993, *Sol. Phys.*, 148, 1
 Dziembowski, W. A., & Goode, P. R. 1991, *ApJ*, 376, 782
 ———. 1992, *ApJ*, 394, 670
 ———. 1997, 317, 919
 Dziembowski, W. A., Goode, P. R., Di Mauro, M. P., Kosovichev, A. G., & Schou, J. 1998, *ApJ*, 509, 456
 Goldreich, P., Murray, N., Willette, G., & Kumar, P. 1991, *ApJ*, 370, 752
 Howe, R., Komm, R., & Hill, F. 1999, *ApJ*, 524, 1084
 Kosovichev, A. G. 1995, in *Proc. Fourth SOHO Workshop (ESA SP-376; Noordwijk: ESA)*, 1
 ———. 1996, *ApJ*, 461, L55
 ———. 1999, *AAS Meeting*, 194, 42.01
 Kuhn, J. R. 1988, *ApJ*, 331, L131
 Kuhn, J. R. 1998, in *Structure and Dynamics of the Interior of the Sun and Sunlike Stars*, ed. S. Korzennik & A. Wilson (Noordwijk: ESA), 871
 Kuhn, J. R., Libbrecht, K. G., & Dicke, R. H. 1988, *Science*, 242, 908
 Libbrecht, K. G., & Woodard, M. F. 1990, *Nature*, 345, 779
 Lin, H. 1995, *ApJ*, 446, 421
 Lin, H., & Rimmele, R. R. 1999, *ApJ*, 514, 448
 Pijpers, F. P., & Thompson, M. J. 1994, *A&A*, 281, 231
 Ritzwoller, M. H., & Lavelly, E. M. 1991, *ApJ*, 369, 557
 Schou, J., Christensen-Dalsgaard, J., & Thompson, M. J. 1994, *ApJ*, 433, 389
 Spruit, H. 1998, in *IAU Symp. 185, New Eyes to See Inside the Sun and Stars*, ed. D. W. Kurtz & J. Leibacher (Dordrecht: Kluwer), 103
 Unno, W., Osaki, Y., Ando, H., Saio, H., & Shibahashi, H. 1989, *Nonradial Oscillation of Stars* (Tokyo: Univ. Tokyo Press)
 Woodard, M. F., & Libbrecht, K. G. 1991, *ApJ*, 374, L61